[8]A. B. Kunz, Phys. Rev. (to be published).
[9]K. Codling and R. P. Madden, Phys. Rev. Letters 12, 106 (1964).
[10]A. P. Lukirskii, T. M. Zimkina, and I. A. Brytov, Izv. Akad. Nauk SSSR, Ser. Fiz. 28, 772 (1964) [translation: Bull. Acad. Sci. USSR Phys. Ser. 28, 681 (1964)]. The $4p$ to s transitions occur at higher energy, 143-145 eV, which we also confirm on measurements of the gas.
[11]At least the first member of each series has recently been observed in solid xenon. See R. Haensel, G. Keitel, C. Kunz, and P. Schreiber, Phys. Rev. Letters 22, 398 (1969).
[12]J. W. Cooper, Phys. Rev. Letters 13, 762 (1964).
[13]Y. Onodera, M. Okazaki, and T. Inui, J. Phys. Soc. Japan 21, 2229 (1966).
[14]U. Fano and J. W. Cooper, Rev. Mod. Phys. 40, 441 (1968).

CHARGE-QUANTIZATION STUDIES USING A TUNNEL CAPACITOR

John Lambe and R. C. Jaklevic
Scientific Laboratory, Ford Motor Company, Dearborn, Michigan 48121
(Received 16 May 1969)

A tunnel capacitor is an array of microscopic resistance-capacitance circuits with the resistive element provided by a tunnel junction. Because of their small size, such microcircuits display special properties due to charge quantization. An array of such circuits shows an oscillatory behavior in its capacitance-versus-voltage measurements. A new type of memory effect is found.

This paper is a report of studies based on a new type of solid-state structure. This structure consists of an array of microscopic series resistance-capacitance elements. The resistance element is formed as a tunneling junction between a metal electrode and a small metal droplet. The capacitance element is formed as a highly insulating oxide between the metal droplet and a second metal electrode. The structure contains a large number of such elements and we call it a tunnel capacitor. This structure makes possible the study of the equilibrium states of microscopic capacitors of such size that the addition of a single electron causes a significant voltage change on one of the capacitors. Thus we can examine the physics of such a system in the case where the quantization of charge becomes an important consideration.

Figure 1(b) shows a schematic representation of this device. It should be noted that it closely resembles a structure which was used by Giaever and Zeller[1] to study zero-bias anomalies in tunneling junctions. There is a very important distinction, however. In their case both oxides were thin enough to permit tunneling since they wished to study tunneling currents flowing between the electrodes. This showed that charge quantization produces a large resistive effect at low applied voltages. The experiments we will describe cannot be carried out unless the second oxide is thick enough to block electron tunneling through it.

Before dealing with experimental methods and results, some of the expected properties of the device will be discussed. Consider an equivalent circuit representing a single element of the array as shown in Fig. 1(a). The tunneling junction is represented by a resistance R and a shunt capacitance C_R. The smaller capacitance C_I is not shunted by any appreciable leakage path. The first quantity we wish to consider is the number of electrons on the metal droplet as a function of the applied voltage V. This question involves a straightforward thermodynamic calculation and the result is sketched in Fig. 1(c). We plot $\langle q \rangle$, the expectation value of added charge, versus the applied voltage V. At $T = 0°K$, this plot is a set

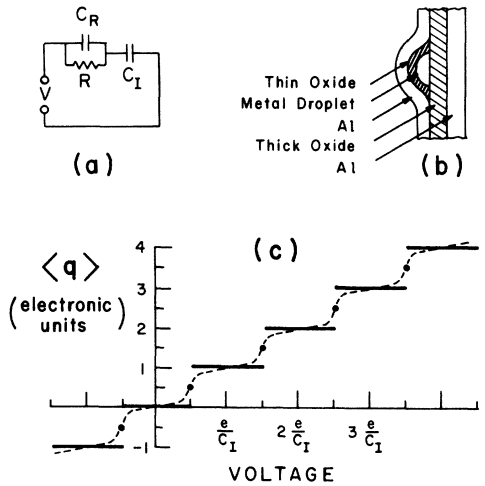

FIG. 1. (a) Schematic of one element of the tunnel capacitor. (b) Structure of the element. (c) Expectation value of added charge on the droplet as a function of the applied voltage V.

of sharp steps. At $T>0°K$ these steps will be rounded, as shown by the dashed curve, and will blend into a straight line as T is increased. In order for the step structure to be present we must consider experiments under the condition

$$kT < \frac{1}{2}\frac{e^2}{C_I + C_R}, \tag{1}$$

where e = electronic charge unit. Note that C_R enters this temperature condition. The period of the steps is given by

$$\Delta V = e/C_I \tag{2}$$

and does not depend on C_R. This period gives a set of applied voltages such that, for an integral number of added charges, the voltage across R (and hence C_R) is zero.

Let a small ac voltage $v\sin\omega t$ be applied to the circuit in addition to the dc voltage V. We then calculate the ac current that would flow in order to furnish the required value of $\langle q\rangle$:

$$\langle i_{ac}\rangle = \frac{d\langle q\rangle}{dt} = \frac{d\langle q\rangle}{dV}\frac{dV}{dt} = \frac{d\langle q\rangle}{dV}\,\omega v\cos\omega t.$$

From this we can define an effective capacitance such that

$$c = d\langle q\rangle/dV.$$

Note that $d\langle q\rangle/dV$ will be an even periodic function of the applied voltage V which can be expanded as a Fourier cosine series. Retaining only the first harmonic,

$$\Delta c = -\alpha\cos(2\pi C_I V/e). \tag{3}$$

In deriving (3) we have oversimplified the actual situation since the effective capacity depends on other circuit parameters. However, this will affect only the magnitude of α and not the period. It is important, however, to consider one additional aspect. We began by assuming that when $V=0$, the electrical potential on the metal droplet was also zero. This need not be the case since in the limit where charge quantization is important, it may be that the Fermi level of the metal droplet cannot "line up" with the Fermi level of the electrodes. We have then in general for the ith capacitor

$$\Delta c_i = -\alpha_i\cos[2\pi C_i(V-V_i)/e]. \tag{4}$$

The term V_i represents a "phase shift" which plays a crucial role in our experiment. We actually measure a parallel array of Δc_i; so the measured capacitance ΔC_M will be

$$\Delta C_M = \sum_i \Delta c_i = -\sum_i \alpha_i\cos[2\pi C_i(V-V_i)/e]. \tag{5}$$

Equation (5) is the central result and will be used to interpret the experimental results.

The experimental structures were prepared by using an aluminum (or tantalum) film upon which a thick oxide was formed by gaseous or solution anodization. This oxide film was in the thickness range 75-500 Å. A small amount of metal (either Pb, Sn, Bi, or In) was evaporated on this to form small metal droplets of about 100 Å diam. These were then oxidized by exposure to room air to give a thin tunneling barrier. A second aluminum electrode was then evaporated over this. For some experiments, this electrode was thin enough to transmit light. The essential results we report could be obtained for any of the group of metal droplets listed above, but we shall show results obtained for indium. The measurement consisted of measuring the total capacitance at a frequency of 100 kHz.

Figure 2 shows the result obtained for a particular structure. The data were taken after the device had been cooled to liquid-helium temperature and maintained at that temperature for an hour. The capacitance was measured as the voltage was scanned uniformly through the voltage range shown. The scanning time was about 30 sec. Note the oscillatory behavior of the curve

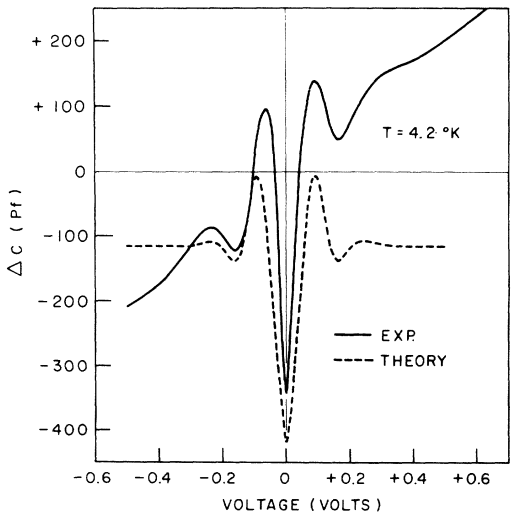

FIG. 2. Measurement of ΔC_M vs V for a device using indium as the metal droplet with average radius approximately 50 Å. The theoretical curve has been displaced downward for clarity and is normalized to the experimental peak at $V=0$.

of ΔC_M vs V. This is a characteristic pattern for all the devices except that the linewidth of the central line and the oscillatory effect vary with the size of the metal droplets and the thickness of the thick oxide. Roughly speaking, the smaller the size of the C_i, the broader the pattern. The magnitude of ΔC_M is about 1% of the total device capacitance. There is also a broad background change. Such background effects are seen in the oxide capacitance even when it is formed with no metal droplets present. We therefore focus attention on changes with respect to this background. The indium droplets become superconducting at lower temperatures but this does not noticeably affect the result.

Figure 3 shows data which illustrates another important aspect of this device. It shows a sequence of measurements made after different steps were carried out. In order to facilitate discussion, we shall refer to the measurement of ΔC_M as a "read" operation. The other operations are referred to as "write." The sample is first cooled to 4.2°K with $V=0$ and the C_M is measured or read. This result, shown in Fig. 3(a), is substantially the same as that shown in Fig. 2. The droplets are larger in this device than those in Fig. 2 so the central line is narrower. At this point the "write" operation is carried out. This consists of applying a voltage or set of discrete voltages for a certain length of time. This can be done while the sample is maintained at 4.2°K or while the sample is warmed up and recooled. The length of time required to produce an effect depends upon relaxation phenomena in the thin oxide and is of the order of a few minutes. One can also use light to accelerate the relaxation process. In the particular example shown in Fig. 3, the writing was carried out by warming the sample to 300°K and slowly cooling while the voltage was switched between the two values indicated in Fig. 3(b). This is done by applying a square voltage wave at a frequency of 1 Hz. The resulting curve of ΔC_M vs V curve shows structure at the two voltage settings. The device thus shows a memory effect of an unusual type. If the voltage is now set to zero and the capacity read from time to time, the memory capacitance slowly fades in magnitude but not in position. The half-life of this memory is typically 15 min at 4.2°K. This effect is observed in all the devices of this type which we have examined. The memory capacitance shows a pattern width which is the same as the pattern initially observed at $V=0$. Also, the induced-memory-capacitance effect at a given voltage grows at the expense of the capacitance effect at $V=0$. The above effects can be observed at 77°K, but they are smaller and the patterns much broader. If the device is warmed to 300°K the memory is erased. The effect has been observed for either polarity and at voltages up to 2 V. In all of the above measurements the reading was done by scanning rapidly so that it did not cause any "write" effects.

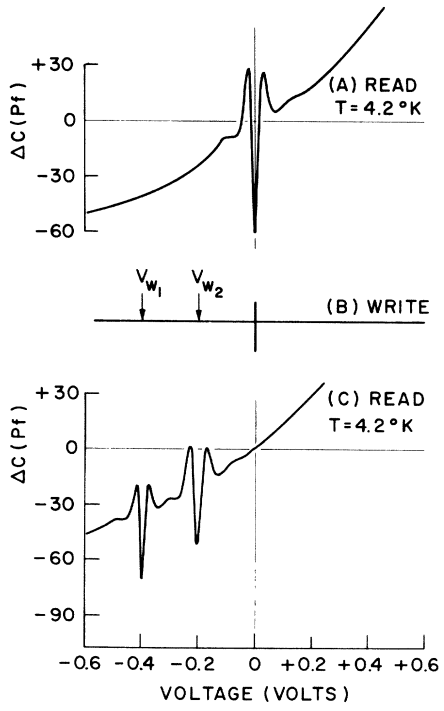

FIG. 3. Measurement of ΔC_M vs V before and after "writing" operation was carried out. Indium droplets of average radius approximately 100 Å.

The effects described in the above experiments can be understood by examination of the phase term V_i in Eq. (5). The experiments can be explained in terms of slow relaxation processes which make the voltage across the thin oxide tend toward zero. For example, these can be of the form of slow polarization changes in each C_R. They can also be due to photoconductive processes if the thin oxide is illuminated during application of the write voltage. If such relaxation processes can occur and if $V=0$ for a long period of time, then all $V_i \cong 0$. Equation (5) then becomes

$$\Delta C_M = -\sum \alpha_i \cos(2\pi C_i V/e), \tag{6}$$

or, using the integral form,

$$\Delta C_M = -\int F(C_i)\alpha_i \cos(2\pi C_i V/e)dC_i, \quad (7)$$

where $F(C_i)$ measures the distribution of microscopic capacitors. Equation (7) is just the Fourier transform of the function $F(C_i)\alpha_i$. If we assign a constant α_i over the distribution of C_i and take a Gaussian distribution for C_i we then have

$$\Delta C_M = -\exp[-(\pi\beta/e)V]^2 \cos[2\pi\bar{C}_i V/e], \quad (8)$$

where $\bar{C}_i$ and β are the average value and distribution width, respectively, of C_i. In this case ΔC_M will be an exponentially damped cosine function as shown in Fig. 2. Equation (8) is plotted in Fig. 2 for particles of 100-Å radius and a distribution width of 50 Å. In this case $\bar{C}_i$ was estimated to be 10^{-6} pF. The particle sizes are consistent with electron-micrograph measurements. No detailed measurement of particle size distribution was attempted, however. The magnitude of the observed ΔC_M effect is in reasonable agreement with the theory if the effect of all the circuit parameters are considered.

The memory-capacitance effect can be understood as a direct consequence of the phase term. Suppose that the metal droplets indeed line up in potential at zero when $V=0$ for a long period of time. Then let a "write" voltage V_W be applied. In general, electrons will be added to the droplets very rapidly by tunneling in an attempt to bring the droplets to the same potential as the nearby electrode. Because of charge quantization it can only do this to within a voltage e/C_i, so that small voltages will exist across C_R. The slow polarization process begins again and the Fermi levels slowly become aligned. This means the "phase term" V_i is changed and at equilibrium is given by

$$V_i = V_W - (ne/C_i), \quad (9)$$

where n is the number of electrons which brings the droplet potential as close as possible to the nearby electrode potential. Then we have

$$\Delta C_M = -\sum \alpha_i \cos\left[2\pi C_i \frac{(V - V_W - ne/C_i)}{e}\right]$$
$$= -\sum \alpha_i \cos[2\pi C_i (V - V_W)/e]. \quad (10)$$

Equation (10) is very similar to Eq. (6) except for the shift V_W. Thus writing at V_W means we will observe a shift in the capacitance pattern from $V=0$ to V_W. The above expression displays the essential features of the memory effect.

It is important to note that the memory at 200 mV in Fig. 3(c), for example, does not mean something is "charged up" to 200 mV. The memory is contained in the phase relation between the periodic microcapacitors. Thus there is no "decay" along the voltage axis. The fading of memory means a blurring out of this phase relationship. It is not necessary that one has complete "alignment" of the phase of the capacitors in order to see an effect. Any partial alignment will yield an effect. Hence, one can write at several voltages as indicated in Fig. 3(c).

It is clear that the polarization phenomena which cause phase shift may arise in many different ways. We expect such processes to occur in amorphous oxides.[2] Such effects will have relaxation times which can become quite long at low temperatures and which can be affected by light. One can also expect that light could free holes and electrons which will produce similar polarization effects when they are retrapped. Any detailed discussion of such processes is, of course, beyond the scope of a brief communication. We merely emphasize that such processes are known to exist and we have shown that they play an essential role in this experiment. It is important that such effects be sufficiently slow, or turned on and off as in the photoeffect situation, if charge quantization effects are to be observed at all. Thus the tunnel junction plays the essential role of providing a sufficiently rapid mechanism of quantized charge transfer so that one can carry out the experiment. It is interesting to speculate as to what role the Josephson effect[3] would play in this case. Unfortunately junctions of the area used here would probably be thermally unstable with respect to Josephson tunneling.[4]

In summary then we have carried out a study of the properties of "simple" RC circuits in the limit of charge quantization. The observed oscillatory behavior of the capacitance of such circuits with respect to applied voltage has been predicted. It has been shown that one can sense and adjust the phase of such oscillatory phenomena.

We wish to thank E. Schermer and R. Ager for their technical assistance. We are indebted to P. Maker and A. W. Overhauser for valuable discussions.

[1]I. Giaever and H. R. Zeller, Phys. Rev. Letters 20,

1504 (1968).
[2]J. M. Stevels, in Non-Crystalline Solids, edited by V. D. Frechette (John Wiley & Sons, Inc., New York, 1960), p. 412.
[3]B. D. Josephson, Phys. Letters 1, 251 (1962).
[4]P. W. Anderson, in Lectures on the Many-Body Problem, edited by E. R. Caianiello (Academic Press, Inc., New York, 1964), Vol. 2, p. 113.

THEORY OF INELASTIC ELECTRON-SURFACE-PLASMON INTERACTIONS IN METAL-SEMICONDUCTOR TUNNEL JUNCTIONS*

K. L. Ngai, E. N. Economou, and Morrel H. Cohen
The James Franck Institute and Department of Physics, The University of Chicago, Chicago, Illinois 60637
(Received 25 April 1969)

The excess tunneling current due to electron–surface-plasmon interactions in semiconductor-metal tunnel junctions is calculated. The expression for the second derivative of this excess current, which corresponds to structure in d^2I/dV^2 as an increase in conductance at bias voltages near the surface plasmon energy in the semiconductor, agrees with experiment both in magnitude and line shape.

Recent studies of n-type GaAs-Pb surface-barrier tunnel junctions by Tsui[1] have shown evidence for the observation of surface-plasmon excitation in a degenerate semiconductor. Structure is observed in d^2I/dV^2 which corresponds to an increase in conductance at bias voltages near the surface-plasmon energy in GaAs. The bias position of the broad peak structures is strongly dependent on the electron concentration of the GaAs electrode. These measurements led Tsui to explain his observations as due to the excitation of surface plasmons (SP) in GaAs by tunneling electrons. Here we present a theoretical model based on Tsui's idea of SP excitation and amenable to quantitative calculation. The magnitude of the change in conductance induced by electron-SP interaction is in agreement with experiment as is the line shape. In addition, it helps to clarify some puzzling features of the observations.[1]

We idealize the semiconductor-metal junction as consisting of semiconductor (S) and metal (M), both semi-infinite, separated by a dielectric medium (I).[2] Their dielectric functions are taken to be of the form[3] $\epsilon_S(\omega)=\epsilon_\infty(1-\omega_S^2/\omega^2)$, $\epsilon_M(\omega)=1-\omega_M^2/\omega^2$, and $\epsilon_I(\omega)=\epsilon_\infty$ ($\epsilon_\infty=11.3$ and $m^*=0.07$ for GaAs[3]). The dispersion relation for surface-plasma oscillations has been calculated with inclusion of retardation effects (i.e., coupling of longitudinal Coulomb fields with transverse electromagnetic ones)[4] and is shown in Fig. 1. The mode described by the upper branch corresponds to oscillations in the M-I interface for large $\vec{p}_\parallel$ (the SP wave vector parallel to the interfaces). The initial sections of this branch are near the curves $\omega=c\epsilon_\infty^{-1/2}p_\parallel$ and $\omega^2=(c^2/\epsilon_\infty)p_\parallel^2+\omega_S^2$, and hence are oscillations of very small amplitude with no physical importance as has been discussed by one of us.[5] Consequently, for frequency range $\omega\sim\omega_S$, the upper mode does not exert any effect and can be neglected. The lower branch describes modes of primary importance. The dispersion is linear for $p_\parallel\ll k_S\equiv\omega_S/c$, i.e., $\omega=\bar{c}p_\parallel$ with

$$\bar{c}=c[d_i/(d_i+\lambda_M+\lambda_S)\epsilon_\infty]^{1/2},$$

$1/\lambda_M=\omega_M/c$, and $1/\lambda_S=\omega_S/c$. This is reminiscent of the SP modes that gave rise to Fiske steps in Josephson junctions.[6] When $p_\parallel\ll k_S$, the mode corresponds to oscillations in the S-I interface and can be adequately described by

$$\frac{\omega}{\omega_S}=\frac{\omega_1+i\omega_2}{\omega_S}=\frac{1}{\sqrt{2}}[1-\exp(-2p_\parallel d)]^{1/2}+i\frac{1}{2\tau\omega_S}, \quad (1)$$

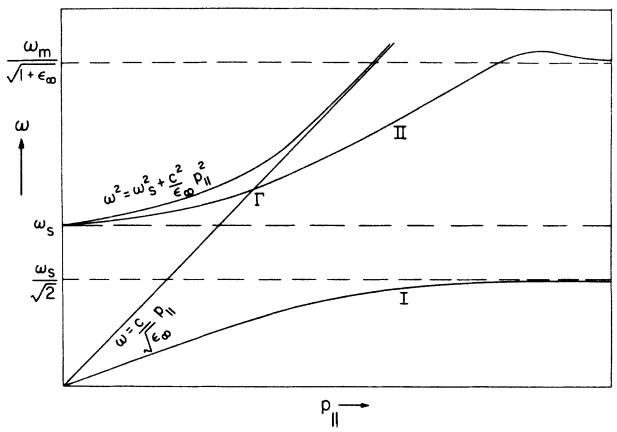

FIG. 1. Schematic dispersion relation for surface-plasmon oscillations in an idealized metal-semiconductor junction (see text). Γ corresponds to a frequency $\sim(\omega_M\omega_S)^{1/2}$.